Supplementary Information (SI) for Catalysis Science & Technology.
This journal is © The Royal Society of Chemistry 2026

Supporting Information

Cobalt-Doped $ZnIn_2S_4$ for Highly Efficient Photocatalytic Oxidation of 5-Hydroxymethylfurfural to 2,5-Diformylfuran

Xiaohan Xing[a], Xu Tang[a], Zhi Zhu[a, b*],Binrong Li[c*], Yixuan Liu[b], Wenhua Xue[b], Pengwei Huo[a], Jun Zhao[b*]*

[a] Institute for Advanced Materials, School of Chemistry and Chemical Engineering, Jiangsu University, Zhenjiang 212013, China

[b] Applied Research Centre for Pearl River Delta Environment, Department of Biology, Hong Kong Baptist University, Hong Kong SAR, China

[c] National and Local Joint Engineering Laboratory of Municipal Sewage Resource Utilization Technology, School of Environmental Science and Engineering, SuzhouUniversity of Science and Technology, Suzhou, 215009, China

****Corresponding authors:***

X.Tang (tangxu@ujs.edu.cn), B. Li (libr@usts.edu.cn), Z.Zhu (zhuzhi@hkbu.edu.hk), J. Zhao (zhaojun@hkbu.edu.hk);

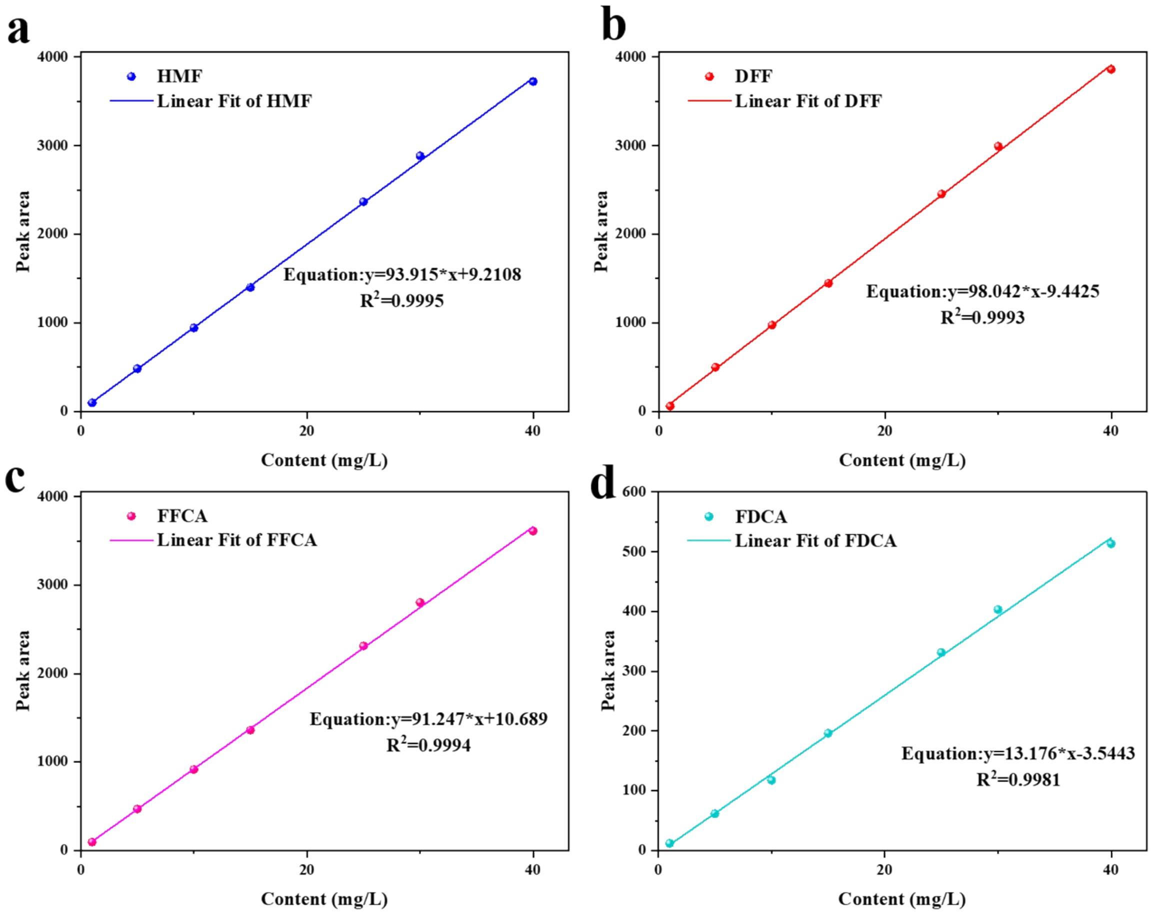

Figure S1. The standard curve for the calibration of : (a) HMF; (b) DFF; (c) FFCA; (d) FDCA.

Quenching Experiment: In order to further understand the photocatalytic mechanism of Co/ZIS-2, in same reaction conditions, different sacrificial agents were added for trapping experiments, such as Triethanolamine (TEOA) as hole scavenger, benzoquinone (BQ) as $\cdot O_2^-$ scavenger, and Furfuryl alcohol (FA) as $^1O_2$ scavenger.

Determination of H_2O_2 concentration: The H_2O_2 concentration was measured by a traditional cerium sulfate $Ce(SO_4)_2$ titration method based on the mechanism that a yellow solution of Ce^{4+} can be reduced by H_2O_2 to colourless Ce^{3+}. Thus, the concentration of Ce^{4+} before and after the reaction can be measured via the UV-vis spectrophotometer. The absorption peak used for the measurement was 316 nm.

$$2Ce^{4+} + H_2O_2 \rightarrow 2Ce^{3+} + 2H^+ + O_2$$

Therefore, the concentration of H_2O_2 can be determined by equation

$$M = \frac{1}{2} \times MCe^{4+}$$

where $M_{Ce}{}^{4+}$ is the mole of consumed Ce^{4+}.

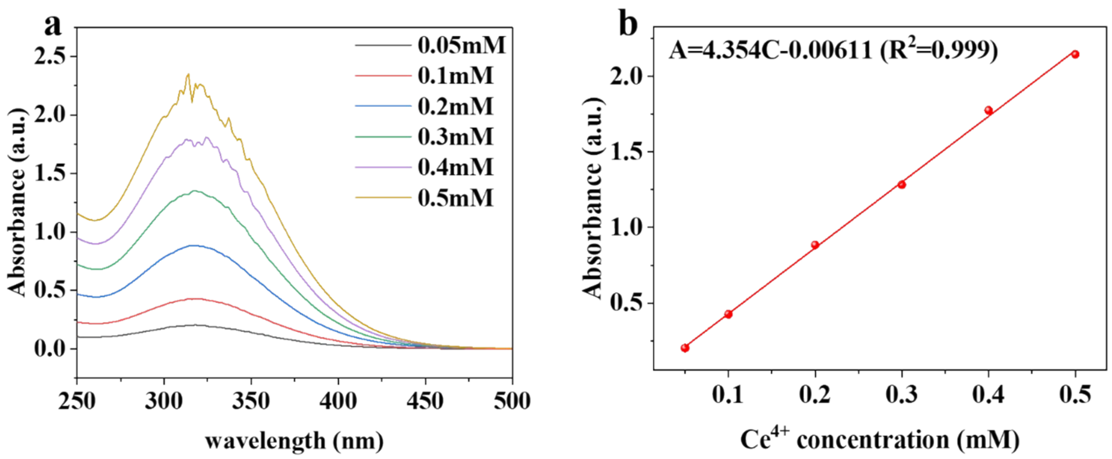

Figure S2. (a) UV–Vis Absorption Spectra of Ce^{4+} Solutions at Various Concentrations; (b) Standard curves at the 316 nm absorption peak.

Electrochemical measurement

Photoelectrochemical tests were performed on the electrochemical workstation CHI660E using the classical three-electrode mode, where in the three-electrode setup, the electrolyte is a 0.5 M Na_2SO_4 aqueous solution, the reference electrode is an Ag/AgCl electrode (saturated KCl), and the counter electrode is a Pt plate. The working electrodes for photocurrent and electrochemical impedance spectroscopy (EIS) were prepared by adding 0.05 g of photocatalyst and 0.01 g of PVP to 3 mL of ethanol, dispersing them homogeneously, adding 0.03 ml of oleic acid, and sonicating for 2 h, after which the dispersions were spin-coated onto 1.0 cm^2 indium-tin-oxide (ITO) substrates.

Density Functional Theory computation details

All the density functional theory (DFT) calculations were performed for structural optimization as implemented in the Vienna Ab-initio Simulation Package (VASP). The PBE exchange-correlation function of the generalized gradient approximation (GGA) was used to describe the exchange correlation energy. A plane-wave kinetic-energy cutoff of 400 eV and a maximum force tolerance of 0.05 eV/Å were employed to obtain well-converged results. A vacuum thickness of 20 Å was used in the z-direction to avoid interactions between periodic slab images.

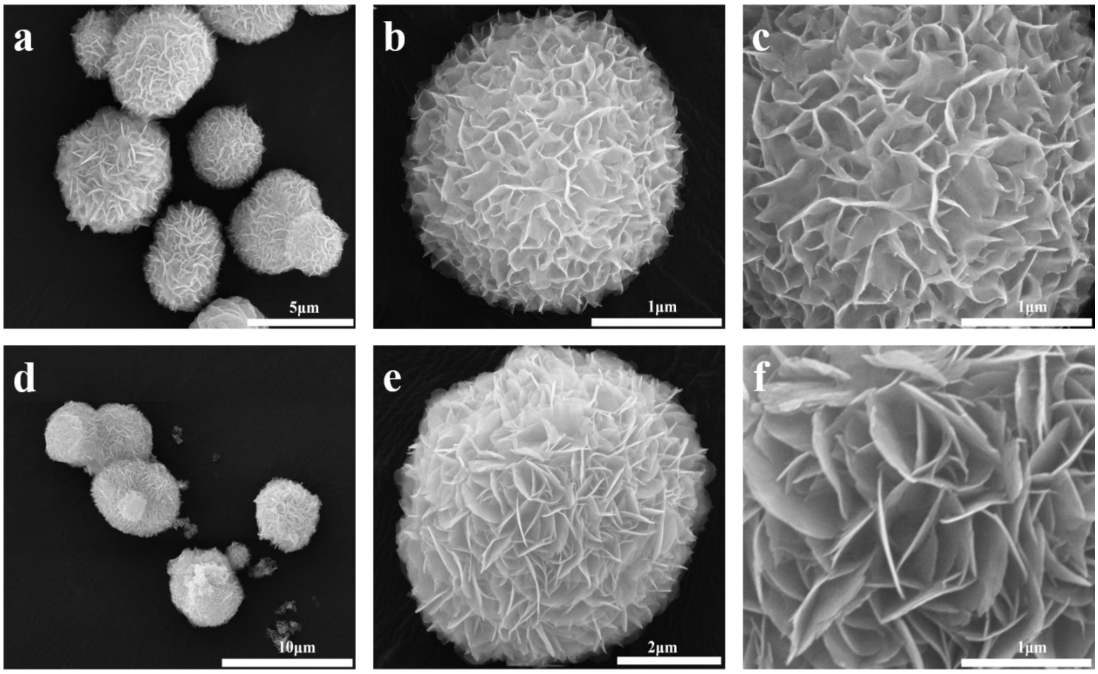

Figure S3. (a-c) SEM image of $ZnIn_2S_4$; (d-f) SEM image of Co/ZIS-2.

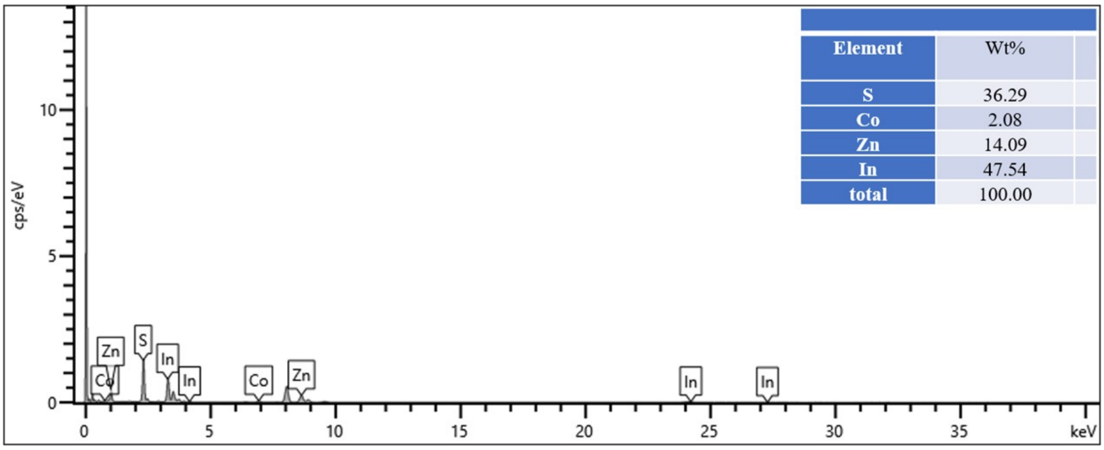

Element	Wt%
S	36.29
Co	2.08
Zn	14.09
In	47.54
total	100.00

Figure S4. Elemental mapping image of Co/ZIS-2

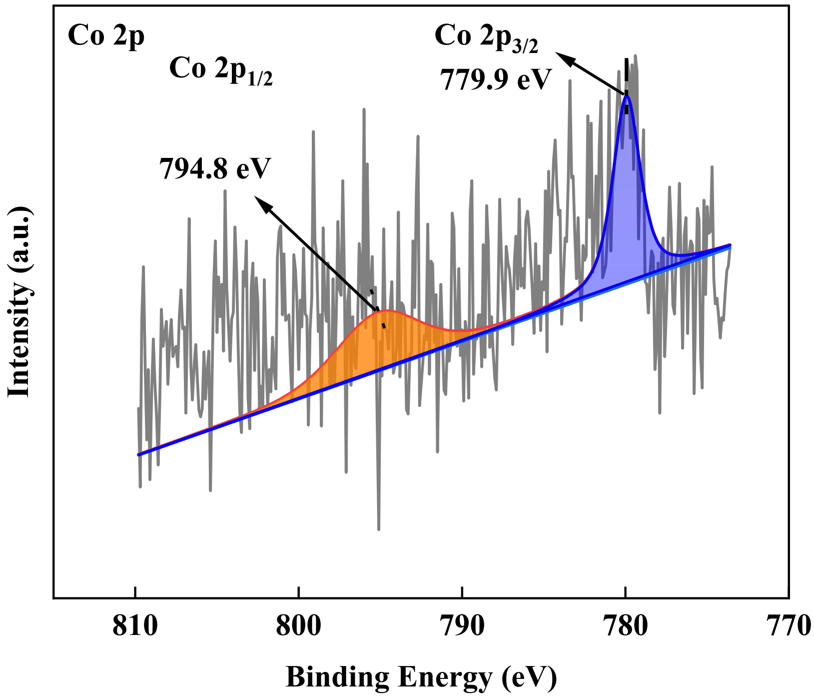

Figure S5. XPS spectrum of Co

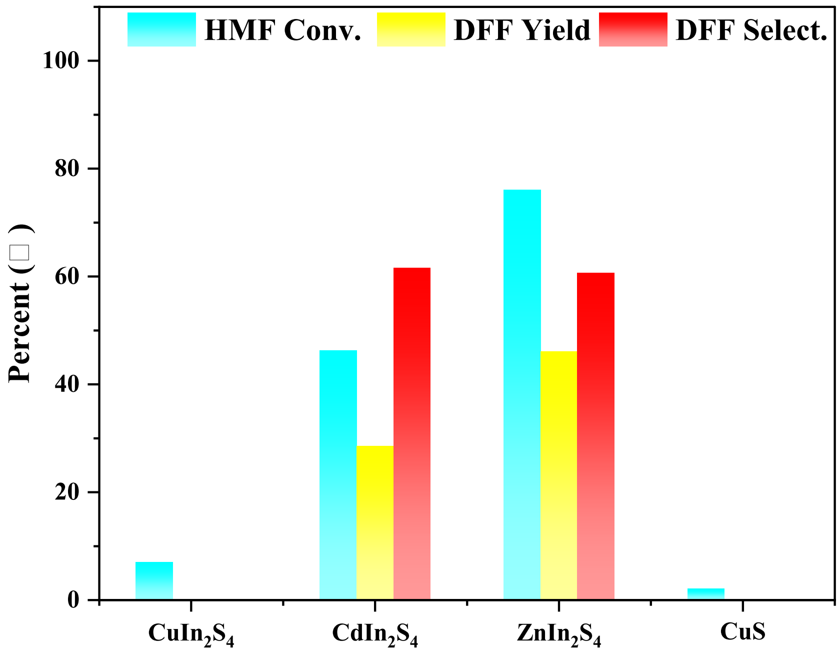

Figure S6. Photocatalytic HMF oxidation activity of different metal sulfides. Reaction conditions: 10 mM HMF, 20 mg catalyst, 20 °C

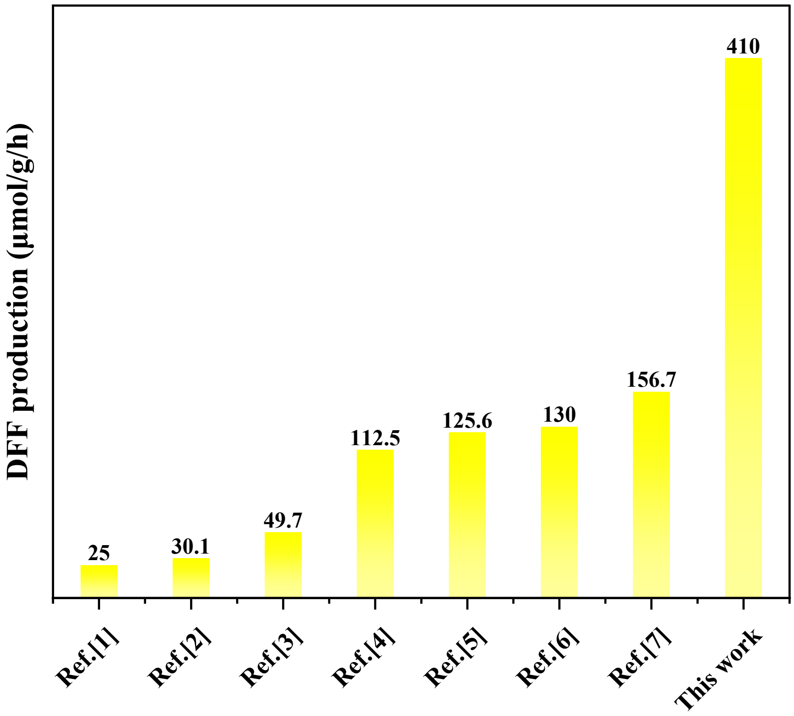

Figure S7. Comparison of photocatalytic DFF production performance in air conditions with some reported photocatalysts.

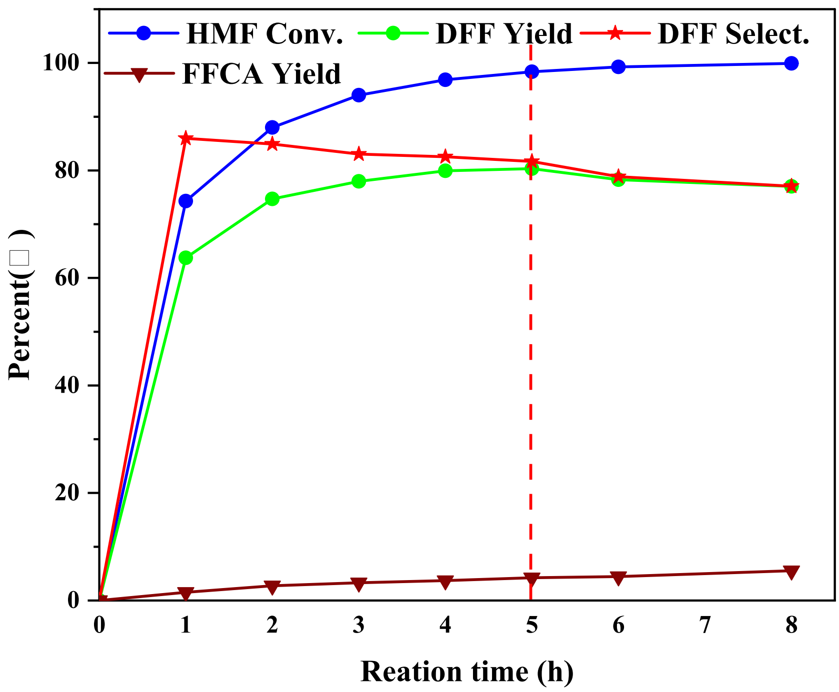

Figure S8. Kinetic plot of Co/ZIS-2.

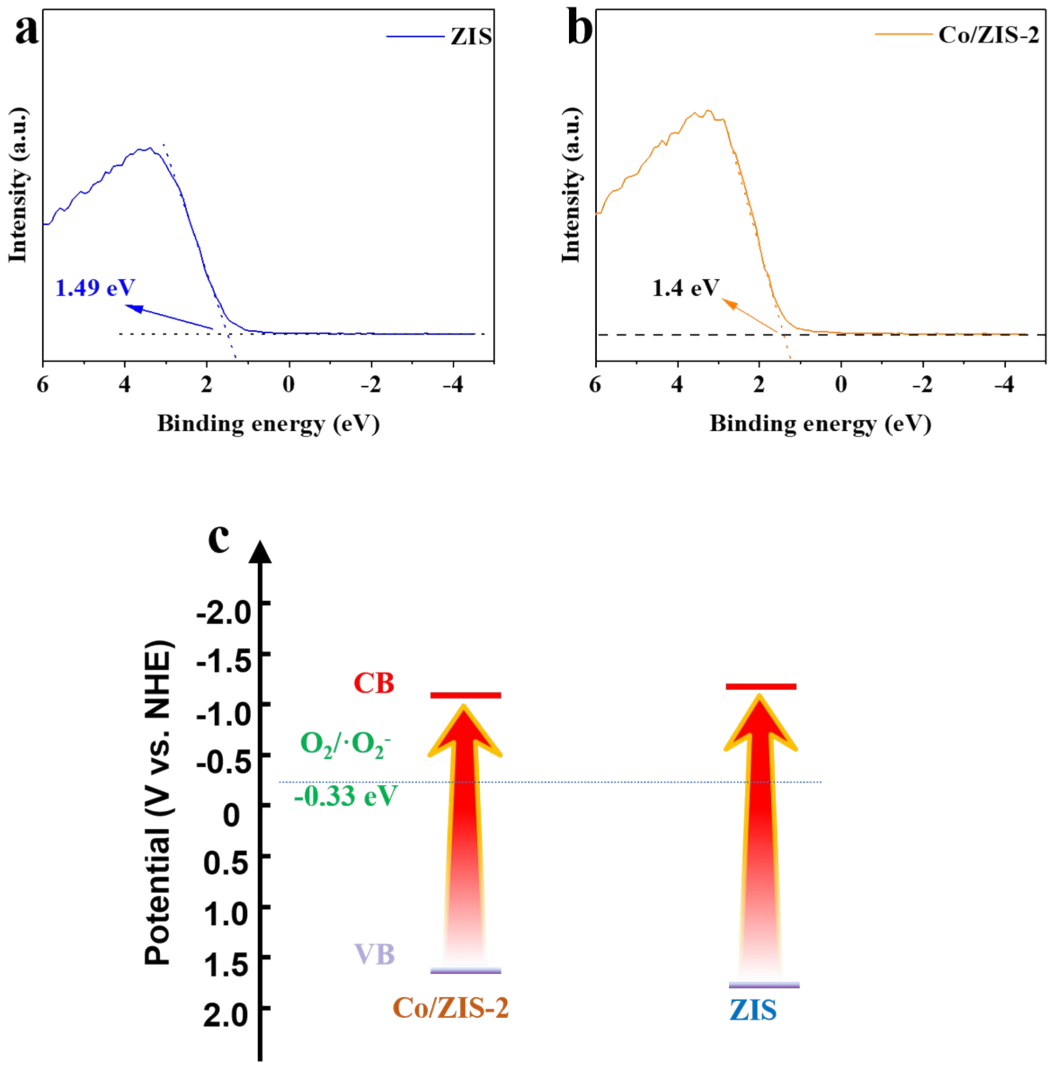

Figure S9. (a) XPS valence band spectra of ZIS; (b) XPS valence band spectra of Co/ZIS-2; (c) The schematic band structure diagrams of ZIS and Co/ZIS-2 are presented.

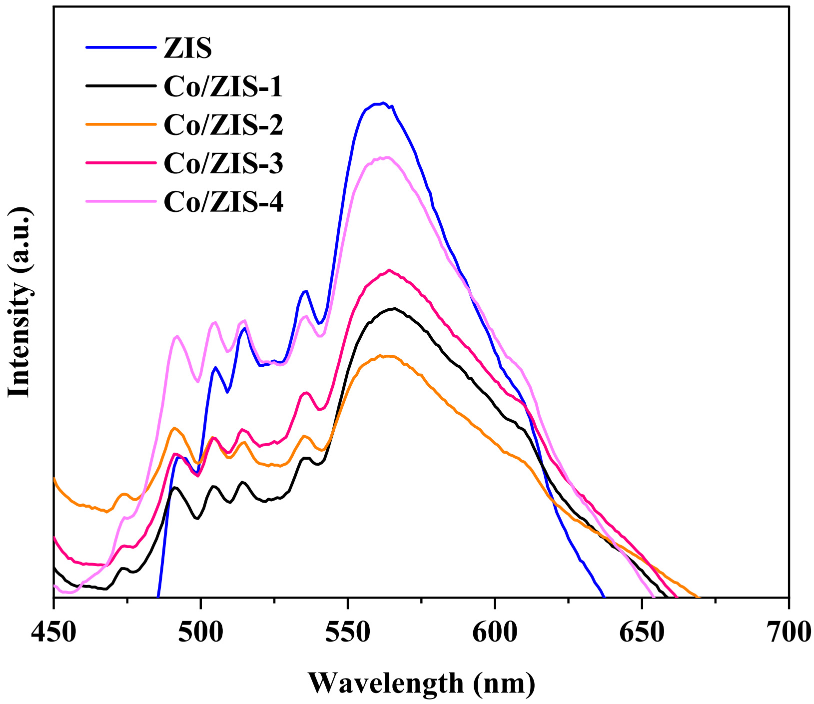

Figure S10. Steady-state PL spectra.

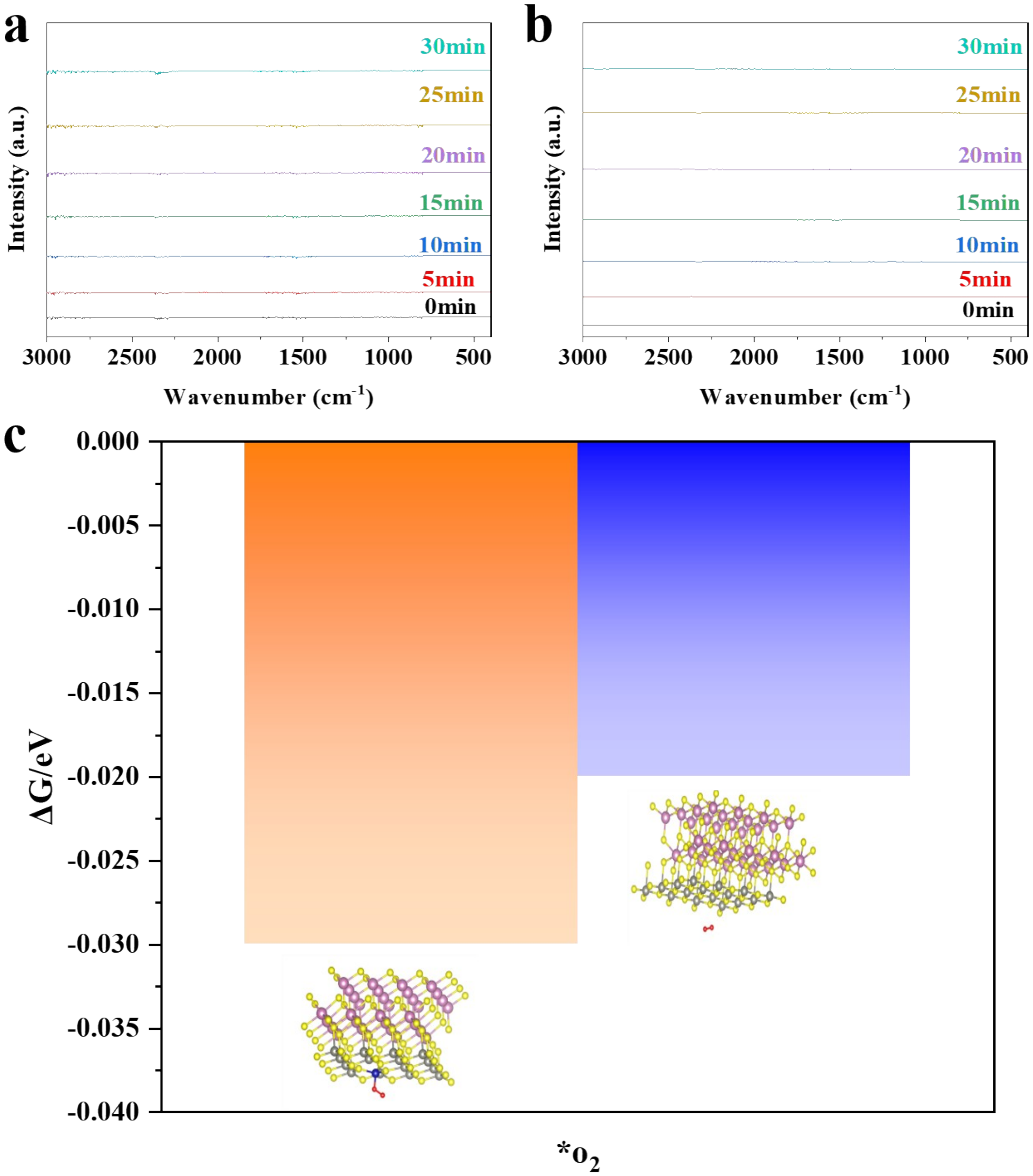

Figure S11. In situ infrared spectra of oxygen adsorption for ZIS and Co/ZIS-2. (a) ZIS. (b) Co/ZIS-2. (c) The DFT calculations of the adsorption energies of oxygen on ZIS and Co/ZIS-2.

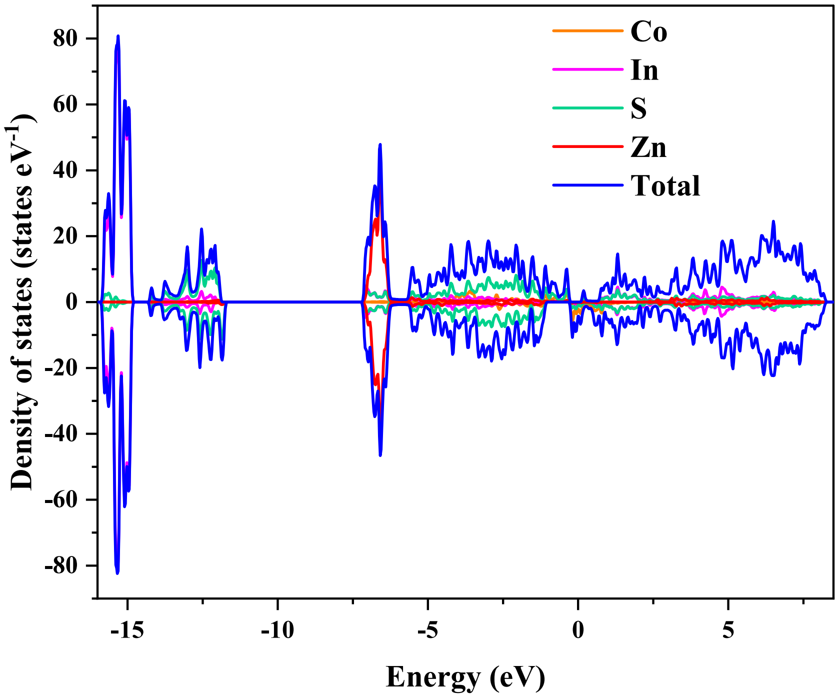

Figure S12. TDOS and Co, Zn, S, O, In PDOS of Co/ZIS-2.

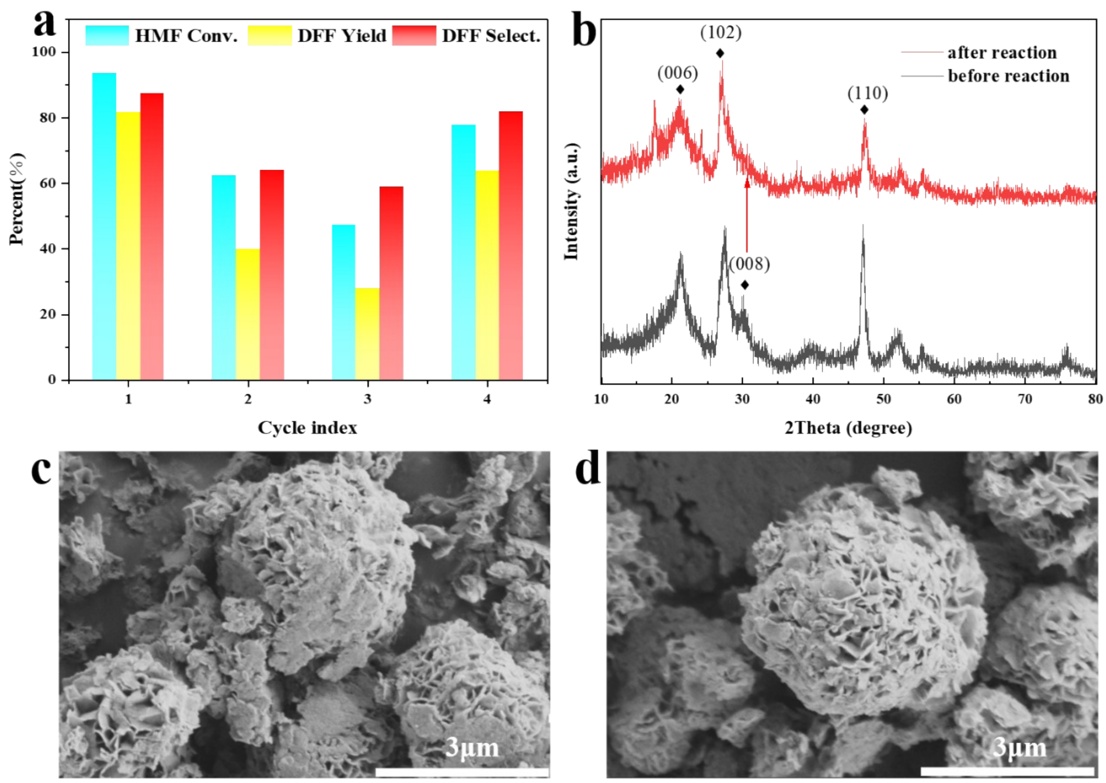

Figure S13. (a) Cycle times activity of Co/ZIS-2, (b) The XRD pattern of the used Co/ZIS-2 is presented; (c-d) SEM topography of Co/ZIS-2 recovery samples.

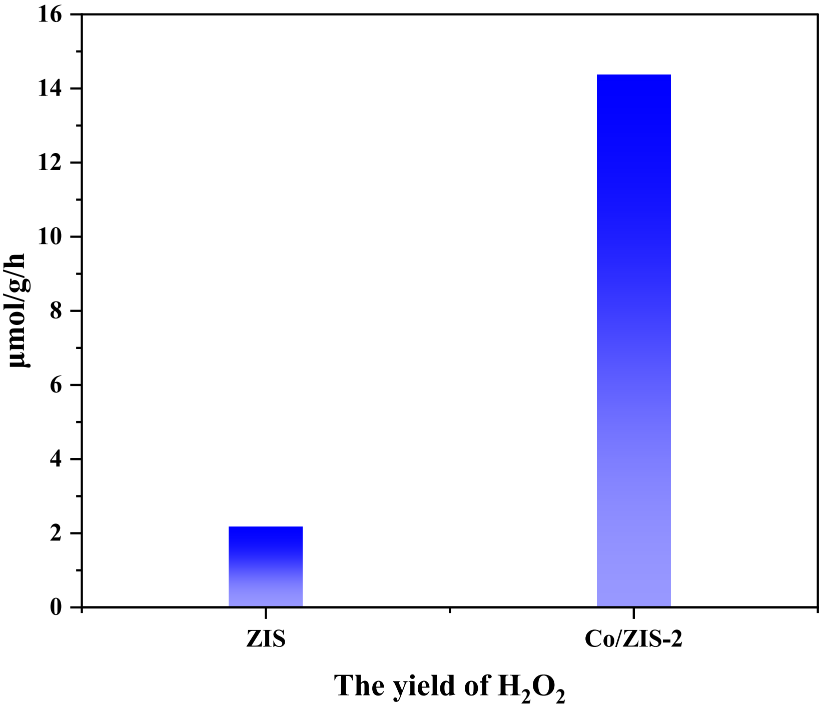

Figure S14. The yield of H_2O_2 (5h).

Some raw data

Sample:Co/ZIS-2
Before the reaction starts
Reaction conditions: No scavengers

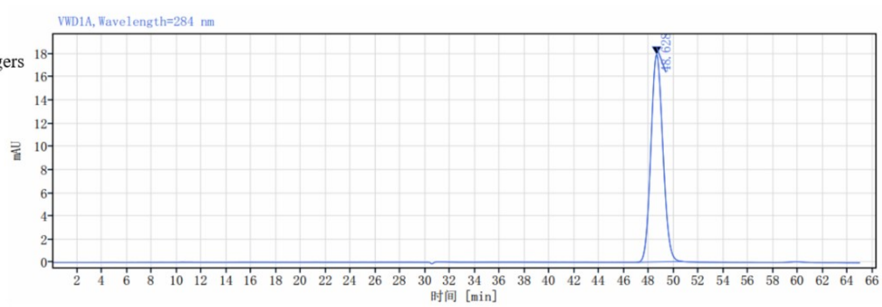

VWD1A, Wavelength=284 nm

Retention time (min)		width (min)	area	Height	
48. 628	BB	3. 64	1199. 06	17. 86	100. 00
		Total	1199. 06		

Figure S15. HPLC chromatogram of HMF before the reaction.

Sample:Co/ZIS-2
After the reaction
Reaction conditions: oxygen

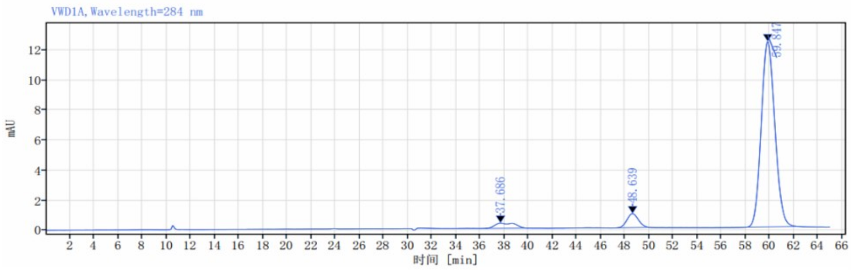

VWD1A, Wavelength=284 nm

Retention time (min)		width (min)	area	Height	
37.686	MM m	1.35	39.30	0.34	3.68
48.639	MM m	0.78	60.60	0.93	5.67
59.847	BB	4.27	968.93	12.32	90.65
		Total	1068.83		

Figure S16. HPLC test diagram of HMF and DFF after reaction.

Calculate result：

Co/ZIS-2	Figure3c						
	Oxygen						
peak area	HMF	DFF	HMF mmo	DFF mmol	Conv.	Yield	Selec.
	1199.06		10.04633				
	60.6	968.93	0.433898	7.767533	95.68	80.04	83.66

Figure S17. Calculate result.

Sample:Co/ZIS-2
Before the reaction starts
Reaction conditions: No scavengers

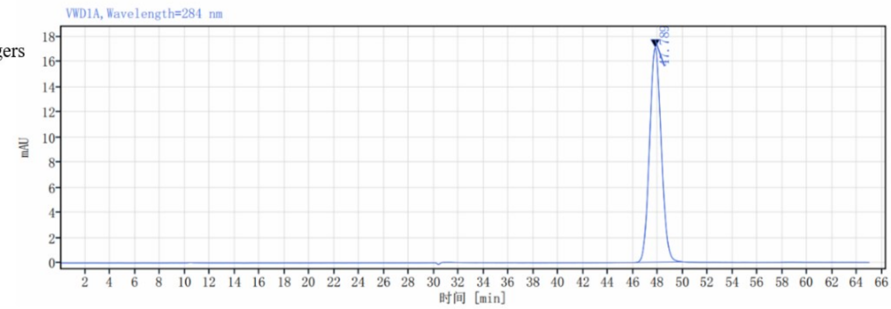

VWD1A, Wavelength=284 nm

Retention time (min)		width (min)	area	Height	
47.789	BB	3.67	1116.56	17.03	100.00
		Total	1116.56		

Figure S18. HPLC chromatogram of HMF before the reaction.

Sample:Co/ZIS-2
After the reaction
Reaction conditions: No scavengers

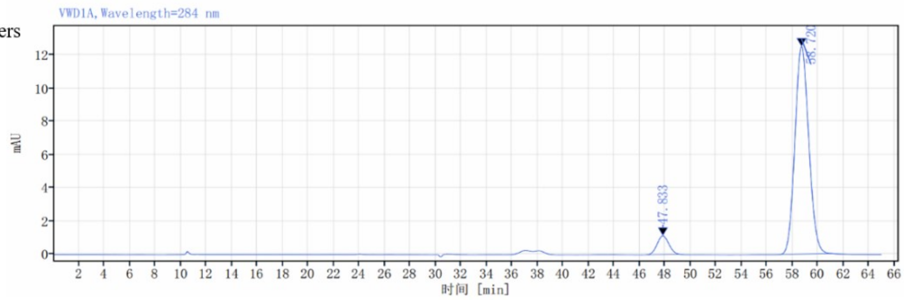

VWD1A, Wavelength=284 nm

Retention time (min)		width (min)	area	Height	
47.833	MM m	0.75	71.57	1.13	7.01
58.720	BB	4.05	949.27	12.52	92.99
		Total	1020.83		

Figure S19. HPLC test diagram of HMF and DFF after reaction.

Calculate result：

Co/ZIS-2	Figure3d						
	No scavenger						
peak area	HMF	DFF	HMF mmo	DFF mmol	Conv.	Yield	Selec.
	1116.56		9.349752				
	71.57	949.27	0.526521	7.879973	94.37	84.28	89.31

Figure S20. Calculate result.

Sample:Co/ZIS-2
Before the reaction starts
Reaction conditions: In ACN

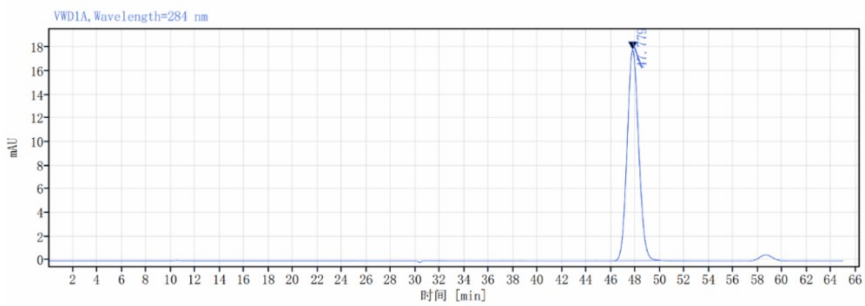

VWD1A, Wavelength=284 nm

Retention time (min)		width (min)	area	Height	
47.779	BB	3.75	1167.34	17.81	100.00
		Total	1167.34		

Figure S21. HPLC chromatogram of HMF before the reaction.

Sample:Co/ZIS-2
After the reaction
Reaction conditions: In ACN

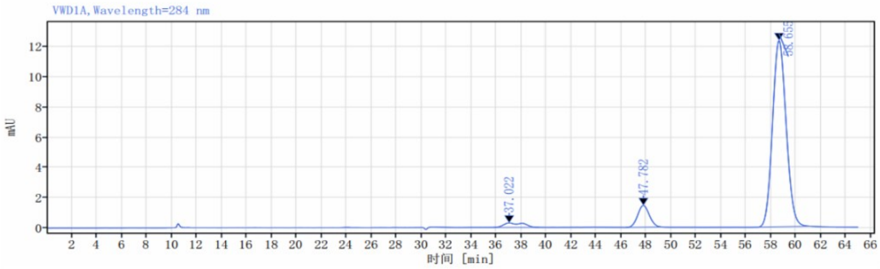

VWD1A, Wavelength=284 nm

Retention time (min)		width (min)	area	Height	
37.022	MM m	1.31	32.63	0.29	3.07
47.782	MM m	0.78	93.13	1.44	8.77
58.655	BB	4.25	935.59	12.32	88.15
		Total	1061.35		

Figure S22. HPLC test diagram of HMF and DFF after reaction.

Co/ZIS-2	Figure3e						
	In ACN						
peak area	HMF	DFF	HMF mmo	DFF mmol/	Conv.	Yield	Selec.
	1167.34		9.778506				
	93.13	935.59	0.70856	7.767533	92.75	79.43	85.64

Figure S23. Calculate result.

Reference

1. Zhu, Q.; Zhuang, Y.; Zhao, H.; Zhan, P.; Ren, C.; Su, C.; Ren, W.; Zhang, J.; Cai, D.; Qin, P. 2,5-Diformylfuran Production by Photocatalytic Selective Oxidation of 5-Hydroxymethylfurfural in Water Using $MoS_2/CdIn_2S_4$ Flower-like Heterojunctions. *Chinese J. Chem. Eng*. 2023, 54, 180–191. DOI: 10.1016/j.cjche.2022.04.018.
2. Qian, H.; Hou, Q.; Zhang, W.; Nie, Y.; Lai, R.; Ren, H.; Yu, G.; Bai, X.; Cai, D.; Ju, M. Construction of Electron Transport Channels and Oxygen Adsorption Sites to Modulate Reactive Oxygen Species for Photocatalytic Selective Oxidation of 5-Hydroxymethylfurfural to 2,5-Diformylfuran. *Appl. Catal. B: Environ*. 2022, 319, 121907. DOI: 10.1016/j.apcatb.2022.121907.
3. Cui, J.; Yu, Z.; Sun, L.; Zhang, M.; Guo, M.; Xiong, J.; Qiao, Y.; Zhang, R.; Lu, X. Photocatalytic Selective Oxidation of Biomass-derived 5-Hydroxymethylfurfural to 2,5-Diformylfuran under Ambient Conditions over $CdIn_2S_4/g\text{-}C_3N_4$ Heterojunctions. *Catal. Sci. Technol*. 2023, 13, 5892–5901. DOI: 10.1039/d3cy00794d.
4. Zhang, M.; Li, Z.; Xin, X.; Zhang, J.; Feng, Y.; Lv, H. Selective Valorization of 5 Hydroxymethylfurfural to 2,5 Diformylfuran Using Atmospheric O_2 and $MAPbBr_3$ Perovskite under Visible Light. *ACS Catal*. 2020, 10, 14793−14800. DOI: 10.1021/acscatal.0c04330.
5. Zhang, M.; Zhang, Y.; Ye, L.; Liu, R.; Qiao, Y.; Sun, L.; Cui, J.; Lu, X. In Situ Fabrication of Ti_3C_2Fx MXene/$CdIn_2S_4$ Schottky Junction for Photocatalytic Oxidation of HMF to DFF under Visible Light. *Appl. Catal. B: Environ*. 2023, 330, 122635. DOI: 10.1016/j.apcatb.2023.122635.
6. Khan, A.; Goepel, M.; Kubas, A.; Łomot, D.; Lisowski, W.; Lisovytskiy, D.; Nowicka, A.; Colmenares, J. C.; Gläser, R. Selective Oxidation of 5-Hydroxymethylfurfural to 2,5-Diformylfuran by Visible Light-Driven Photocatalysis over In Situ Substrate-Sensitized Titania. *ChemSusChem*. 2021, 14, 1351–1362. DOI: 10.1002/cssc.202002687.
7. Guo, Y.; Gong, M.; Xu, X.; Dong, Y.; Wang, G. Efficient Photocatalytic Selective Oxidation of 5-Hydroxymethylfurfural on $Bi_{24}O_{29}Br_{10}(WO_4)_2$ Solid Solution via Enhanced Charge Separation. *Catal. Sci. Technol*. 2025, DOI: 10.1039/d4cy01420k.